



Cite this: *Chem. Commun.*, 2015, 51, 2159

Received 7th November 2014,  
Accepted 17th December 2014

DOI: 10.1039/c4cc08898k

www.rsc.org/chemcomm

## Bioimaging of the microRNA-294 expression-dependent color change in cells by a dual fluorophore-based molecular beacon†

Hae Young Ko,<sup>‡ab</sup> Jonghwan Lee,<sup>‡ab</sup> Yong Seung Lee,<sup>ab</sup> Ha-Na Gu,<sup>ab</sup> Bahy A. Ali,<sup>cd</sup> Abdulaziz A. Al-Khedhairy,<sup>c</sup> Hyejung Heo,<sup>ab</sup> Sujeong Cho<sup>ab</sup> and Soonhag Kim<sup>\*ab</sup>

**A dual fluorophore-based color-tunable molecular beacon visualized the microRNA-294 expression-dependent color change in cells.**

During embryonic stem cell (ESC) differentiation, the expression of specific mRNAs, proteins and microRNAs (miRNAs, miRs) is affected. miRNAs can induce changes in ESCs by binding and regulating hundreds of genes individually and simultaneously.<sup>1</sup> For imaging miRNA, reporter gene imaging systems based on bioluminescence,<sup>2</sup> fluorescence,<sup>3</sup> magnetic resonance,<sup>4</sup> and radioisotope<sup>5</sup> have been successfully developed. However, these methods are based on a signal-off system. The application range is sometimes limited by its surrounding background signals resulting from autofluorescence, especially when the target gene is expressed at a very low level. A molecular beacon (MB) imaging system to sense miRNAs (miR MB) was developed to overcome the limited applicability of reporter genes.<sup>6</sup> MB is a synthetic oligonucleotide, which consists of a target binding region for RNA, protein or miRNA, a quenching molecule, and a fluorophore at the end of each oligonucleotide.<sup>7</sup> In the absence of a target, the fluorescence signal is absorbed by a quencher as a result of fluorescence resonance energy transfer (FRET) between a fluorophore and a quencher. In the presence of a target, a quencher is separated from MB, resulting in the signal-on imaging signal. In previous studies, we have successfully applied the proof-of-concept of MB to image miRNAs during myogenesis<sup>6a</sup> and neurogenesis<sup>6b</sup> representing signal-on imaging activity in the presence of a miRNA.

Sensing a miRNA by a fluorescence signal from the miR MB is dependent on a single fluorophore, because the structure of the miR MB consisted of a single fluorophore at one end and a quencher at the other end. Such miRNA MBs simply visualize single-fluorophore-dependent signal-on or -off activity in response to miRNA presence. Thus, when the fluorescence intensity of the on/off-tunable miRNA MB is weak in cells, it is hard to obtain accurate information about the expression of target miRNA. To overcome this, a dual fluorophore-based miRNA MB was developed to sense color-tunable visualization of miRNA expression.<sup>8</sup> In this work, to monitor the miRNA expression-dependent color change, miR-294 was selected which is highly expressed in undifferentiated ESCs and affects the cell-cycle of ESCs.<sup>9</sup> We conducted bioimaging of the miR-294 expression-dependent and miR-294-regulating color change before and after neuronal differentiation of P19 (mouse embryonal carcinoma) cells.

We designed a color-tunable miR-294 MB (designated as Color294 MB) to visualize the miR-294 expression-dependent color change in cells. The Color294 MB was a linear structured and a partially double-stranded DNA oligonucleotide (Fig. 1). The long DNA oligonucleotide contained a miR-294 binding sequence and labeled with two types of fluorophores; Cy5 (excitation/emission: 650/670 nm) at the 5' end as a reporter probe and Cy3

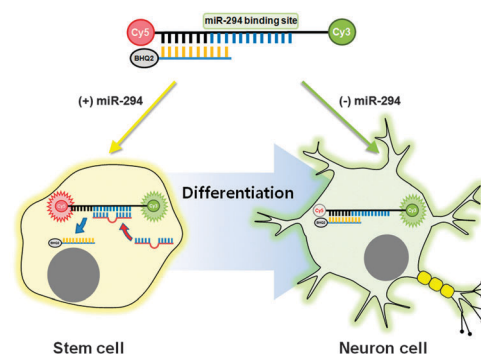


Fig. 1 Schematic diagram of the Color294 MB to sense the miR-294 expression-dependent color change.

<sup>a</sup> Institute for Bio-Medical Convergence, College of Medicine, Catholic Kwandong University, Gangneung-si, Gangwon-do, 270-701, Republic of Korea.

E-mail: kimsoonhag@empal.com; Tel: +82-32-290-2771

<sup>b</sup> Catholic Kwandong University International St. Mary's Hospital, Incheon Metropolitan City, 404-834, Republic of Korea

<sup>c</sup> Department of Zoology, College of Science, King Saud University, Riyadh 11451, Saudi Arabia

<sup>d</sup> Department of Nucleic Acids Research, Genetic Engineering and Biotechnology Research Institute, City for Scientific Research and Technological Applications, Alexandria, Egypt

† Electronic supplementary information (ESI) available. See DOI: 10.1039/c4cc08898k

‡ These authors contributed equally to this work.

(excitation/emission: 546/563 nm) at the 3' end as a reference probe (designated as long oligo). A short DNA oligonucleotide had a partially complementary sequence to the 5' end of the long DNA oligonucleotide and a black hole quencher 2 (BHQ2) at the 3' end (designated as quencher oligo). The long and quencher oligos were partially hybridized with each other and formed the ColoR294 MB. The mechanism for visualizing the miR-294 expression-dependent color change in cells using the ColoR294 MB is provided below. The Cy3 fluorophore (green color) of the reference probe is not influenced by the quencher because of a sufficient distance away from the quencher. Therefore, Cy3 is constantly emitted regardless of miR-294 expression. In the presence of miR-294 before neuronal differentiation of P19 cells, the Cy5 fluorescence signal (red color) of the reporter probe is activated by specific binding of miR-294 to the miR-294 binding region of the long oligo and detachment of the quencher oligo from the ColoR294 MB. As a result, P19 cells before neuronal differentiation are visualized by yellow color due to the merge of green from the reference probe and red from the reporter probe. In the absence of miR-294 after neuronal differentiation of P19 cells, the Cy5 fluorescence signal of the reporter probe is quenched by BHQ2 due to the close proximity between the two. P19 cells are visualized by green from the Cy3 fluorescence signal of the reference probe.

The quantitative and qualitative fluorescence analysis demonstrated that the fluorescence brightness of the reporter probe from the long oligo (10 pmol) was sequentially quenched as the concentration (0, 1, 5, 10 and 20 pmol) of the quencher oligo increased (Fig. 2a and Fig. S1a, ESI†). However, the fluorescence activity of the reference probe was constant regardless of the concentration of the quencher oligo. The reporter probe revealed maximal quenching efficiency (82%) at 10 pmol of the quencher oligo. These results indicate the successful and stable formation of the ColoR294 MB.

To examine the specificity of sensing miR-294 using the ColoR294 MB, four different concentrations (0, 10, 20 and 30 pmol) of an exogenous miR-294 were applied to the ColoR294 MB in a black plate. Both qualitative and quantitative fluorescence analysis showed that Cy5 fluorescence intensity of the reporter probe was gradually brightened by the increase in the concentration of the exogenous miR-294 due to the hybridization of miR-294 to the miR-294 binding region of the long oligo (Fig. 2b and Fig. S1b, ESI†). Meanwhile, the incubation of an exogenous miR-1 (negative control) did not affect the fluorescence recovery of the reporter probe. The Cy3 reference probe of the ColoR294 MB treated with either miR-294 or miR-1 showed no difference in fluorescence brightness. The stability of the ColoR294 MB was confirmed by incubating in PBS and Opti-MEM media up to 4 days. During the 4 days of incubation, consistent quenching efficiency was observed, and in

the presence of exogenous miR-294, the ColoR294 MB showed fluorescence recovery (Fig. S2, ESI†). These results reveal great specificity of sensing miR-294 using the ColoR294 MB.

The qRT-PCR showed that CHO (Chinese hamster ovary) cells rarely expressed miR-294 (Fig. S3, ESI†). CHO cells treated with the ColoR294 MB demonstrated that Cy5 signals of the reporter probe remained in the quenched state in the absence of exogenous miR-294 and in the presence of exogenous miR-1 (30 pmol) (Fig. S4, ESI†). However, the Cy5 fluorescence activities of the ColoR294 MB in CHO cells were gradually and significantly recovered in response to the dose of exogenous miR-294. The Cy3 reference probe of the ColoR294 MB in CHO cells showed constant fluorescence intensity irrespective of incubation with exogenous miR-294 or miR-1. Confocal microscopy imaging analysis demonstrated that the cytoplasm of CHO cells treated with the ColoR294 MB in the absence of the exogenous miR-294 and in the presence of miR-1 was mostly visualized by the green color obtained from the reference probe, showing the quenching of red fluorescence signals from the reporter probe (Fig. 3). The recovery and dose-dependent increase of Cy5 red fluorescence signals from the reporter probe were detected from the cytoplasm of the ColoR294 MB-treated CHO cells with additional incubation of the exogenous miR-294. Green fluorescence brightness of the Cy3 reporter probe in CHO cells was constantly shown regardless of miR-294 and miR-1 transfection. In other words, without miR-294 or with miR-1, the ColoR294 MB-transfected CHO cells were visualized in green color. The presence of miR-294 showed the ColoR294 MB-transfected CHO cells in yellow color by the merging effect between green from Cy3 and red from Cy5. Line scan analysis of the region of interest (ROI) further confirmed that the color change of the ColoR294 MB-treated CHO cells from green to yellow was induced by the miR-294 concentration-dependent red signal recovery. These results indicate the high specificity of color-tunable sensing of miR-294 expression in cells using the ColoR294 MB.

For visualizing the endogenous miR-294-dependent color changes during neurogenesis, P19 cells were treated with retinoic acid (RA) in culture medium to induce neuronal differentiation.

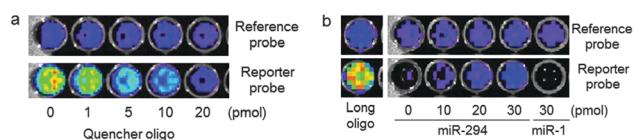


Fig. 2 Fluorescence images for (a) quenching efficiency of the reporter probe in the ColoR294 MB and (b) specificity of the ColoR294 MB for sensing miR-294.

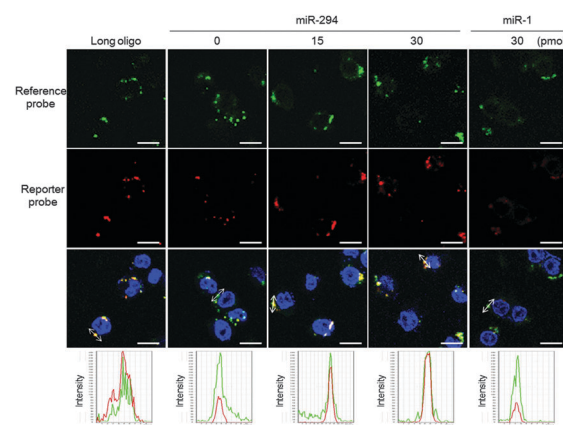


Fig. 3 Confocal microscope images of the ColoR294 MB in CHO cells. Figures in the third row were merged with DAPI. Fluorescence intensity of Cy5 and Cy3 in the fourth row shows the line scan data along the line shown in the third row. All scale bars are 10  $\mu$ m.

Induction of differentiation into neurons was confirmed by immunocyto staining of differentiated P19 cells with the increase in TuJ1 (neuronal marker) expression and the decrease in the Oct4 (stem cell marker) level (Fig. S5, ESI†). The qRT-PCR showed that endogenous miR-294 expression was decreased after neuronal differentiation of P19 cells (Fig. S3, ESI†). To verify whether the expression and function of the miR-294 were affected by the ColoR294 MB itself, we analyzed the endogenous expression levels of miR-294 and the retinoblastoma-like protein 2 (Rbl2) gene, which is an endogenous target of miR-294.<sup>10</sup> Compared with non-treated P19 cells, RT-PCR demonstrated no significant differences in endogenous expressions of miR-294 and Rbl2 in P19 cells transfected with 30 pmol of the ColoR294 MB (Fig. S6, ESI†). These results indicate that the concentration of 30 pmol of the ColoR294 MB was enough to sense an endogenous miR-294 expression during neurogenesis in P19 cells without affecting intact miR-294 expression and function.

Four days after neuronal differentiation of P19 cells transfected with the ColoR294 MB (30 pmol), compared with undifferentiated P19 cells, the Cy5 signal of the reporter probe was decreased in differentiated cells because of lower expression of an endogenous miR-294 in the differentiated state (Fig. S7, ESI†). In addition, when a miR-294 antagomir, which is a synthetic oligonucleotide that fully complements the miR-294 sequence, was co-transfected into undifferentiated P19 cells, Cy5 fluorescence intensity of the reporter probe was significantly decreased, compared with the undifferentiated P19 cells treated with null oligonucleotides, because the miR-294 antagomir inhibited the binding between miR-294 and the ColoR294 MB. And as we expected, the fluorescence signal of the reference probe in P19 cells was constant regardless of neuronal induction and the treatment of the miR-294 antagomir. Similarly, confocal microscope images showed that the constant bright green fluorescence of the Cy3 reference probe was found in the cytoplasm of differentiated P19 cells and undifferentiated P19 cells with and without the treatment of the miR-294 antagomir (Fig. 4). Since the expression of endogenous miR-294 level was higher before neuronal

differentiation, the red fluorescence brightness of the reporter probe was stronger in the cytoplasm of undifferentiated P19 cells than differentiated P19 cells. The additional treatment of the miR-294 antagomir decreased the red fluorescence brightness of the reporter probe in undifferentiated P19 cells due to the inhibition of the detachment of the quencher oligo from the ColoR294 MB. As a result, from the color mixture of the reporter probe with the reference probe, P19 cells transfected with the ColoR294 MB were visualized as yellow before neuronal differentiation and green after neuronal differentiation. The ROI analysis of the line scan analysis further confirmed the fluorescence changes of the Cy5 reporter probe and constant fluorescence signals of the reference probe before and after neuronal differentiation of P19 cells.

miRNAs have attracted considerable interest in stem cell research as a one of the key regulators in differentiation and cell-cycle.<sup>9</sup> We successfully developed a dual fluorophore-based color-tunable molecular beacon to sense miR-294 expression. This color-tunable mechanism of the ColoR294 MB successfully demonstrated that undifferentiated P19 cells that highly expressed miR-294 were visualized by yellow color and differentiated neuronal P19 cells that had decrease in miR-294 expression by greenish color. The ColoR294 MB revealed high specificity to sense miR-294 expression- and miR-294-regulating cellular development-dependent color change. Therefore, the ColoR294 MB would be one of the feasible ways to monitor stem cell population and differentiation during stem cell maintenance and differentiation, and in clinical applications.

This work was supported by the Bio & Medical Technology Development Program of the National Research Foundation (NRF) funded by the Korean government (MEST) (No. 2012-0006097 and 2013R1A2A2A01068140), the Next-Generation BioGreen 21 program (#PJ010002), Rural Development Administration and a grant of the Korean Health Technology R&D Project, Ministry of Health & Welfare (HI14C3297).

## Notes and references

- (a) M. A. Valencia-Sanchez, J. Liu, G. J. Hannon and R. Parker, *Genes Dev.*, 2006, **20**, 515–524; (b) E. Wienholds and R. H. A. Plasterk, *FEBS Lett.*, 2005, **579**, 5911–5922.
- H. Y. Ko, D. W. Hwang, D. S. Lee and S. Kim, *Nat. Protoc.*, 2009, **4**, 1663–1669.
- B. D. Brown, M. A. Venneri, A. Zingale, S. L. Sergi and L. Naldini, *Nat. Med.*, 2006, **12**, 585–591.
- M. Jo, B. A. Ali, A. A. Al-Khedhairi, C. H. Lee, B. Kim, S. Haam, Y. Huh, H. Y. Ko and S. Kim, *Biomaterials*, 2012, **33**, 6456–6467.
- M. Jo, M. S. Jeong, H. Y. Ko, C. H. Lee, W. J. Kang and S. Kim, *Biomaterials*, 2013, **34**, 4803–4809.
- (a) W. J. Kang, Y. L. Cho, J. R. Chae, J. D. Lee, K. Choi and S. Kim, *Biomaterials*, 2011, **32**, 1915–1922; (b) D. W. Hwang, I. C. Song, D. S. Lee and S. Kim, *Small*, 2010, **6**, 81–88; (c) J. K. Kim, K. Choi, M. Lee, M. Jo and S. Kim, *Biomaterials*, 2012, **33**, 207–217.
- (a) X. Fang, J. J. Li, J. Perlette, W. Tan and K. Wang, *Anal. Chem.*, 2000, **72**, 747A–753A; (b) J. J. Li, R. Geyer and W. Tan, *Nucleic Acids Res.*, 2000, **28**, e52; (c) M. B. Baker, G. Bao and C. D. Searles, *Nucleic Acids Res.*, 2012, **40**, e13.
- H. Y. Ko, J. Y. Joo, Y. S. Lee, H. Heo, J. J. Ko and S. Kim, *Sci. Rep.*, 2014, **4**, 4626.
- E. Heinrich and S. Dimmeler, *Circ. Res.*, 2012, **110**, 1014–1022.
- R. Benetti, S. Gonzalo, I. Jaco, P. Muñoz, S. Gonzalez, S. Schoeffner, E. Murchison, T. Andl, T. Chen, P. Klatt, E. Li, M. Serrano, S. Millar, G. Hannon and M. A. Blasco, *Nat. Struct. Mol. Biol.*, 2008, **15**, 268–279.

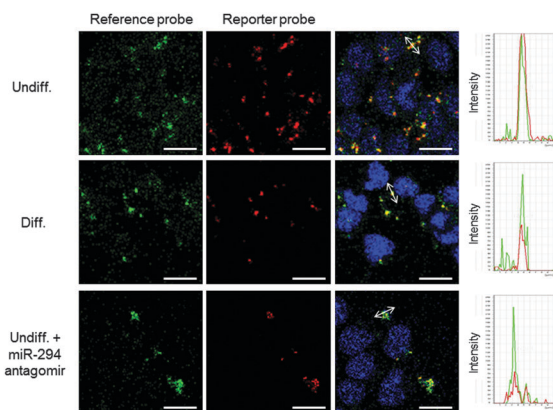


**Fig. 4** Confocal microscope images of the ColoR294 MB during neuronal differentiation of P19 cells. Figures in the third column were merged with DAPI. Fluorescence intensity of red and green in the fourth column shows the line scan data along the line shown in the third column. All scale bars are 10  $\mu$ m.